JOURNAL OF CATALYSIS 98, 468–476 (1986)

A Transient Kinetic Observation of Chain Growth in the Fischer–Tropsch Synthesis

XUEZHI ZHANG AND PAUL BILOEN[1]

Chemical and Petroleum Engineering Department, University of Pittsburgh, Pittsburgh, Pennsylvania 15261

Received June 13, 1985; revised November 19, 1985

An abrupt change of the reaction environment from $^{12}CO/H_2$ to $^{13}CO/H_2$ leads to a gradual ingrowth of ^{13}C in hydrocarbons. This rate of ingrowth can be modeled in a manner which is essentially independent of the details of the reaction mechanism. It is calculated that the rate of C–C bond formation varies from $\geq 1\ s^{-1}$ (ruthenium) to $\leq 0.1\ s^{-1}$ (cobalt). Further findings include the experimental observation of surface heterogeneity and the relatively short residence times for the C_1 monomers involved in chain growth.

INTRODUCTION

There have been numerous studies in recent years addressing mechanistic aspects of the Fischer–Tropsch (F–T) synthesis (*1–5*):

$$n\mathrm{CO} + 2n(+1)\mathrm{H_2} \rightarrow \mathrm{C}_n\mathrm{H}_{2n(+2)} + n\mathrm{H_2O}$$

One of the issues which, despite all the research, is still unsettled is the time scale on which the C–C bonds are being formed. This matter has some practical implications. It might, for example, be possible to influence the product distribution by either external cycling of the reaction conditions (*6*) or by the addition of a chain-transfer reagent (*7*), provided that the rate of C–C bond formation is sufficiently slow.

The lack of data on absolute rate (units = s^{-1}) of C–C bond formation essentially derives from the fact that most reaction-rate studies utilize steady-state kinetics techniques. For a single elementary step, involving intermediates present at coverage θ and exhibiting a lifetime k^{-1}, the reaction rate (TOF) can be expressed by (*8–10*)

$$\mathrm{TOF} = k \cdot \theta,$$

where k is reactivity of the intermediates (s^{-1}). It is apparent that a (steady state) measurement of TOF does not allow for the separate assessment of k and θ.

The foregoing statement can be made somewhat more specific. Whereas the full details of the elementary reaction steps are not known, an "overall" sequence of events leading to chain growth has been well established (*11*). The experimentally observed Schulz–Flory distribution of chain lengths:

$$\frac{\%\ \text{mole}\ \mathrm{C}_n}{\%\ \text{mole}\ \mathrm{C}_{n-1}} = \alpha \qquad (1)$$

is indicative of a sequence of independently repeated additions of C_1 groups to the growing chain, C_n, competing with the termination step

$$\mathrm{C}_{n-1}{}^* \xrightarrow[+\,\mathrm{C_1}]{k_p} \mathrm{C}_n{}^* \xrightarrow[+\,\mathrm{C_1}]{k_p} \mathrm{C}_{n+1}{}^*$$
$$\mathrm{C}_n{}^* \xrightarrow{k_t} \mathrm{C}_n(\mathrm{g})$$

The steady-state condition for θ_{C_n} yields

$$\frac{dC_n^*}{dt} = 0 = k_p\theta_{C_{n-1}} - (k_p + k_t)\theta_{C_n}.$$

Hence:

$$\frac{\theta_{C_n}}{\theta_{C_{n-1}}} = \frac{k_p}{k_p + k_t} = \alpha \qquad (2)$$

Equation (2) yields (1) via:

$$\mathrm{TOF}_{C_n} = k_t \cdot \theta_{C_n}. \qquad (3)$$

[1] To whom all correspondence should be addressed.

0021-9517/86 $3.00

It can be seen that steady-state rates (3) give only the *product*, $k \cdot \theta$, and that the steady-state product distribution (2) gives only the *ratio*, k_p/k_t. Neither of them is capable of giving values for the "absolute" (i.e., formally first order, units $= s^{-1}$) rate constants k_p and k_t. This limitation of steady-state kinetics has been well documented (*12–15*). Accordingly it is a nonsteady-state kinetic method (*9*, *16*) that has been utilized in the presently reported research to measure "absolute" values for k and θ of surface intermediates in the F–T reaction.

Dautzenberg *et al.* (*17*) and Kieffer (*18*), both using step-concentration transients, have addressed rates of C–C bond formation. Dautzenberg found C–C bond formation over Ru to be slow (of the order of 0.017 s^{-1}), whereas Kieffer concluded that the C–C bond formation over Fe is quite fast. The problem with step-concentration transients in F–T, and particularly those which involve a variation in the ratio H_2/CO, is that they might lead to nontypical surface chemistry, such as hydrogenolysis and/or conversion of accumulated by-products (*2*, *5*, *22*).

More recently two preliminary studies appeared (*9*, *20*) of the nonsteady-state type, utilized in this report. They employ an abrupt switch in the *isotopic* composition of the reaction atmosphere from $^{12}CO/H_2$ to $^{13}CO/H_2$. As a result, a transient kinetic phenomenon is being observed: the gradual ingrowth of ^{13}C in the hydrocarbon chains (cf. this paper, Figs. 1–5). This nonsteady-state phenomenon allows for the observation of rates of chain growth at conditions which are representative of the steady state. Biloen *et al.* performed a preliminary study (*9*) which did not yet allow the detection of "mixed" transients such as $^{12}C_{n-i}{}^{13}C_iH_{2n}$, and also suffered to some extent from chromatographic effects (cf. Results). Accordingly, only lower limits for the rates of C–C bond formation could be given. At the prevailing conditions the rate of C–C bond formation ranged from ≥0.014

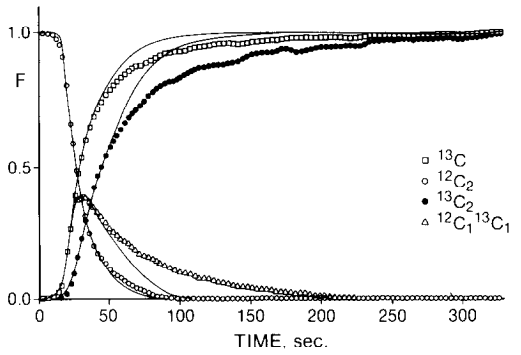

FIG. 2. The transients of C_1 and C_2 species. In addition to the separate data points, the full curves give the results of the model calculations (cf. Fig. 7 and Data Analysis under Results). The conditions are shown in the caption for Fig. 1. Catalyst: cobalt.

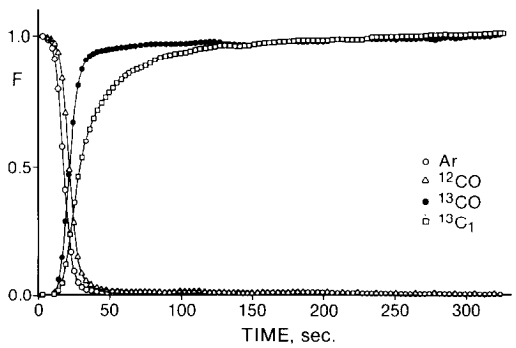

FIG. 1. Transients of Ar, CO, and CH_4 corresponding to a switch from ^{12}CO to ^{13}CO. Catalyst: cobalt. T = 210°C, P = 1 bar, D_2/CO = 3.

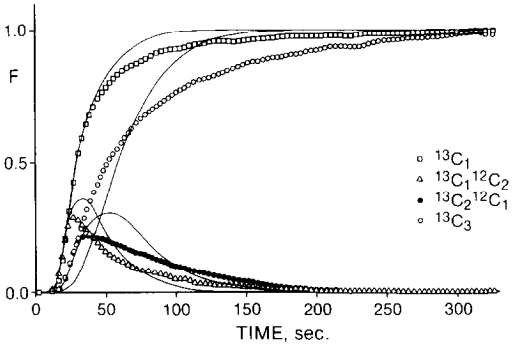

FIG. 3. The transients of C_1 and C_3 species. In addition to the separate data points, the full curves give the results of the model calculations (cf. Fig. 7 and Data Analysis under Results). Catalyst: cobalt. The conditions are shown in the caption for Fig. 1.

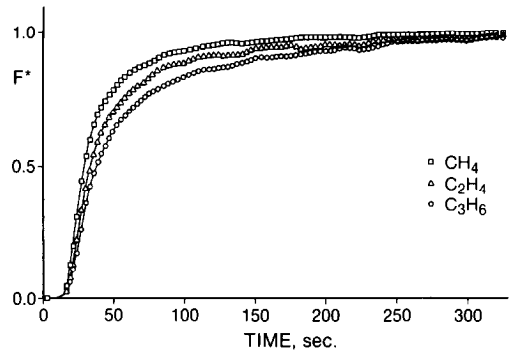

FIG. 4. The transients of ^{13}C in C_1, C_2, and C_3 over cobalt. The conditions are shown in the caption for Fig. 1.

s^{-1} (Ni) via ≥ 0.05 s^{-1} (Co) to ≥ 0.5 s^{-1} (Ru). Mims and McCandlish (*20*) used the same method in conjunction with an incisive analytical technique: ^{13}C NMR. Focusing on Fe, they inferred from the lack of anisotropy in the position of ^{13}C in the product $^{13}C_i$ $^{12}C_{4-i}$ H_8 that C–C bond formation takes place at a rate exceeding 1 s^{-1}.

We presently report on the isotopic transients obtained with ruthenium and cobalt catalysts. On-line mass spectrometry combined with adequate data acquisition allows the resolution of all transients in the C_2–C_3 products. These transients have been analyzed in detail, which leads to the lifetimes and coverage of several of the key surface intermediates.

EXPERIMENTAL

Preparation of the catalysts. (1) Unsupported Co was prepared by precipitation from a 10% solution of $Co(NO_3)_2$ by Na_2CO_3. The suspension was heated to 110°C. The precipitate was filtered off and washed with boiling deionized water until a brown ring test showed that no nitrate was left in the filtrate. The precipitate was dried at 110°C for 12 hr, crushed, and sieved to −200 mesh. Then it was physically mixed with SiO_2 beads (mesh size −100 + 120) in a ratio of 1:3. Finally, the preparation was reduced at 350°C for 12 hr in flowing hydrogen (8 nl/h) over 0.5 g catalyst. It has an exposed cobalt surface area equivalent to 1 ml(STP) CO/g catalyst, as determined from $^{12}CO/^{13}CO$ exchange at 100°C.

(2) Ru/Al_2O_3 was prepared by dry impregnation of γ-Al_2O_3 with $RuCl_3$. Reduction was carried out in flowing hydrogen at 300°C for 2 h. The catalyst has an exposed ruthenium surface area equivalent to 5 ml(STP) CO/g catalyst, as determined from $^{12}CO/^{13}CO$ exchange at 100°C. An amount of 0.5 g catalyst was used in the experiment.

The experiments were carried out in a plug-flow reactor with internal diameter of 3.2 mm. An upstream four-way valve allowed abrupt switching from ^{12}CO to ^{13}CO, or vice versa. Brooks mass flow controllers and Tescom backpressure regulators ensured that partial pressures were essentially unaffected by the isotopic switch. The maximum CO conversion was 15%.

On-line mass spectrometry was performed by sampling continuously the reactor outlet. A small part of the outlet stream was routed via a 100-μm-i.d. heated capillary and a Varian flow-by valve into an Extra Nuclear Model 2750-50 quadrupole mass spectrometer, which was housed in a permanently baked (100°C) UHV-compatible vacuum chamber. This chamber was pumped by a 90 liters/s Leybold–Heraeus turbomolecular pump.

The intensities of selected masses were collected continuously with an Apple IIe

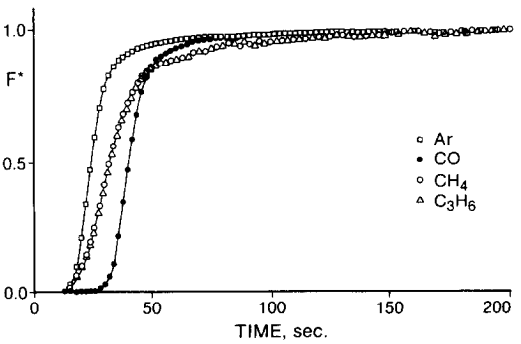

FIG. 5. The transients of Ar, CO, and the ingrowth of ^{13}C in C_1 and C_3 over ruthenium. T = 210°C, P = 1 bar, D_2/CO = 3.

TABLE 1

Selected Masses

Species	Mass
$^{13}CD_4$	21
$^{12}C_2D_4$	32
$^{12}C_1{}^{13}C_1D_4$	33
$^{13}C_2D_5$	36
$^{12}C_3D_5$	46
$^{12}C_2{}^{13}C_1D_5$	47
$^{12}C_1{}^{13}C_2D_7$	52
$^{13}C_3D_7$	53

microcomputer, utilizing a Cyborg-Isaac interface. In order to minimize the interference from fragments of hydrocarbons such as C_4, the open electron-impact ionizer was operated at an impact energy of only 22 eV. The residual fragmentation, however, is still significant. Table 1 lists the selected masses for the species under investigation. For the convenience of detecting the transients of $^{12}C_{n-i}{}^{13}C_i$, D_2 is used instead of H_2 (*10*).

In conjunction with MS analysis, gas chromatography was used to analyze the steady-state reactor effluent stream. The product was separated by a Poropak Q column in series with a 80/100 Carbopak C/0.2% Carbowax 1500 using a He carrier flow of 20 cm^3/min. The steady-state product distribution is close to an Anderson–Schulz–Flory one, with an approximately 15% excess in CH_4 and an approximately 20% undershoot in C_2H_4.

RESULTS

In response to the abrupt change in reaction environment from $^{12}CO/D_2$ to $^{13}CO/D_2$ the isotopic composition (i.e., i in $^{12}C_{n-i}{}^{13}C_i$) of the hydrocarbon products changes gradually. These responses were measured with on-line MS (cf. Experimental) and plotted in two different representations:

$$F(^{12}C_{n-i}{}^{13}C_i) = \frac{[^{12}C_{n-i}{}^{13}C_i]}{\sum_{i=0}^{n} [^{12}C_{n-i}{}^{13}C_i]}$$

and

$$F^*[^{13}C \text{ in } C_n] = \frac{1}{n} \sum_{i=0}^{n} i \cdot F(^{12}C_{n-i}{}^{13}C_i)$$

with $[^{12}C_{n-i}{}^{13}C_i]$ being a measure for the concentration of species i. The inspection of the experimental data reveals that the transients closely obey

$$\sum_{i=0}^{n} F(^{12}C_{n-i}{}^{13}C_i) = 1$$

which is a reflection of

$$\sum_{i=0}^{n} [^{12}C_{n-i}{}^{13}C_i] = \text{constant}.$$

Figures 1–4 show the transients measured over the Co catalyst at $D_2/CO = 3$, $T = 210°C$, and $P = 1$ bar. Separated data points have been displayed together with full curves which correspond to model predictions (cf. below). Figure 5 represents the transients over Ru at $D_2/CO = 3$, $T = 210°C$, and $P = 1$ bar.

When switching off ^{12}CO and Ar (as a tracer) simultaneously at the reactor inlet, there is a time delay between the disappearance of ^{12}CO and Ar at the reactor outlet (Figs. 1 and 5). This front-elution, chromatographic separation is due to desorption in $^{13}CO/D_2$ atmosphere of an inventory of $^{12}CO_{ad}$, which is not paralleled by desorption of a reservoir of Ar_{ad} (*9, 21*). This effect was utilized routinely to determine *in situ* the number of surface-exposed cobalt and ruthenium atoms. All coverages, θ, quoted in this paper have been calculated from the amount of CO (ml(STP)) observed upon $^{12}CO/^{13}CO$ exchange over the fresh catalyst at 100°C and a ratio $H_2/CO = 3$, assuming CO/Co = 0.8.

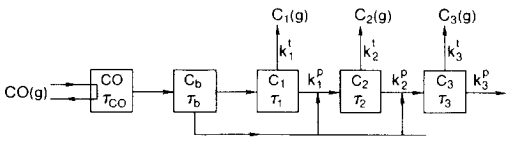

FIG. 6. Network of interconnected pools of surface intermediates, underlying the modeling.

The chromatographic effect should be kept sufficiently small, in order to avoid interference with the intrinsic kinetics (*9*). In practice the chromatographic effect is considered to be negligible when the area between the Ar and ^{12}CO curve is less than 20% of that between Ar and $^{13}CH_4$. By working at sufficiently high space velocity (around 1000 liters/liter/h) this condition could be met with cobalt (Fig. 2). With ruthenium, however, the reactions are faster, and the reservoir of adsorbed CO is larger. Accordingly, the shape of the transients is dominated by the chromatographic effect (cf. Fig. 5 of this paper with Fig. 12 of (*9*)), and only upper limits for lifetimes of intermediates could be abstracted (Table 3). Steady-state kinetic data for cobalt i.e., TOF's and values for the chain-length distribution parameter α, have been listed in Table 2.

Data Analysis

As discussed in the Introduction, the steady-state product distribution indicates chains to grow in independent, unidirectional steps:

$$C_n + C_1^b \rightarrow C_{n+1} \qquad (4)$$

The model utilized in this paper and shown in Fig. 7 is compatible with Eq. (4). Adsorbed CO has a lifetime τ_{CO} before it converts to a surface intermediate C_1^b or desorbs to CO in the gas phase. Surface intermediates C_1^b will either convert to C_1 or they will add to C_n ($n = 1, 2, \ldots$).

TABLE 2

TOF's and α's at Different D_2/CO Ratios

Catalyst: Co, T = 210°C, P = 1 bar				
D_2/CO	1	1.64	3.27[a]	6.55
$TOF_1 \times 10^{-3}$, s^{-1}	2.23	3.11	4.83	8.64
$TOF_2 \times 10^{-3}$, s^{-1}	1.76	1.68	1.58	1.33
$TOF_3 \times 10^{-3}$, s^{-1}	1.43	1.33	1.04	0.72
$TOF_t \times 10^{-3}$, s^{-1}	5.42	6.12	7.45	9.97
α	0.65	0.61	0.52	0.41

[a] [Olefin]/[paraffin] = 3.2 (C_2), 1.4 (C_3), and 1.2 (C_4).

TABLE 3

Transient over Ru/Al_2O_3: Upper Limits for the Lifetime of Surface Intermediates

	Catalyst: Ru/Al_2O_3
D_2/CO	3
T	210°C
P	1 bar
TOF	4×10^{-2} s^{-1}
α	0.65
Data	Fig. 5
τ_b	≤1.5 s
τ_1	≤0.5 s
τ_2	≤0.3 s
τ_3	≤0.3 s
$k_p = \alpha/\tau_2$	≥1 s^{-1}

Additional assumptions are:

(a) Except CO_{ad}, H_{ad}, $C_{1\,ad}^b$, and C_{n-ad} no other intermediates exhibit significant θ and τ values.

(b) Each pool of intermediates is internally homogeneous, i.e., characterized by only two parameters: an abundance (θ) and lifetime (τ).

Mass balance for the pool of surface intermediates C_n leads to

$$\frac{dN_i}{dt} = N\frac{dF_i}{dt} = R(F_{in} - F_i)$$

in which N equals the number of intermediates C_n; R the rate of production and consumption of intermediates C_n; N_i the number of intermediates with constitution $^{12}C_{n-i}$ $^{13}C_i$; F_{in} the value of N_i/N in the *inlet* to the pool C_n; and F_i the value of N_i/N of the pool C_n (and of the outlet of the pool).

Thus,

$$\frac{dF_i}{dt} = \frac{1}{\tau}(F_{in} - F_i)$$

with

$$\tau = \frac{N}{R}.$$

Upon substitution:

$$F_i = F' \cdot e^{-t/\tau},$$

where F' is an unknown function of t to be determined, it is obtained that

$$\frac{dF'}{dt} = \frac{1}{\tau} e^{t/\tau} \cdot F_{in}. \quad (5)$$

The expression for F_{in} is, when $n \geq 2$,

$$F_{in} = F(^{12}C_{n-1-i}{}^{13}C_i) \cdot F(^{12}C_b) + F(^{12}C_{n-i}{}^{13}C_{i-1}) \cdot F(^{13}C_b)$$

whereas

$$F(^{12}C_b) = \frac{N^{12}C_b}{N_b}$$

$$F(^{13}C_b) = \frac{N^{13}C_b}{N_b}.$$

For pool C_b,

$F_{in} = F(^{12}CO)$ for ^{12}C-containing species,

$F_{in} = F(^{13}CO)$ for ^{13}C-containing species.

For pool C_1,

$F_{in} = F(^{12}C_b)$ for ^{12}C-containing species,

$F_{in} = F(^{13}C_b)$ for ^{13}C-containing species.

At this point we mention that isotopes are unique in that they allow for the observation of transient-kinetic phenomena with the system, essentially, at steady state (*9, 15, 16*). In the prevailing context it is ^{12}C and ^{13}C which exhibit essentially the same chemical reactivity. Therefore neither N nor R or τ depend on the isotopic constitution, F_i. Consequently, Eq. (5) can be integrated analytically. For the τ values listed in Table 4 we present the calculated $F_i(t)$ curves in Figs. 2 and 3.

TABLE 4

Lifetime, τ, of Intermediates, as Obtained from Isotopic Transients for Cobalt

Data: Figs. 1–3				
Criterium	τ_b (s)	τ_1 (s)	τ_2 (s)	τ_3 (s)
Computer matching the leading edge of the $F_i(t)$ curves simulations	1.5 ± 1	15 ± 2	15 ± 4	15 ± 4
Matching the total area under the $F_i(t)$ curves	1 ± 4	18 ± 4	15 ± 6	15 ± 8

DISCUSSION

Whereas with cobalt there is a delay between the ingrowth of ^{13}C in CH_4, C_2H_4 and C_3H_6 such a delay is virtually absent in case of ruthenium (cf. Fig. 4 with Fig. 5). In order to quantify this observation we consider in Figs. 4 and 5, the area, A, bounded by the ^{13}C-in-CH_4 and the ^{13}C-in-C_3H_6 curves. This area is of the order 30 s (Co) versus ≤2 s (Ru). The analytical solutions of Eq. (5) allow us to predict this area for any chosen set of parameter values τ_b, τ_1, τ_2, and τ_3. In order to obtain upper limits for the ruthenium case we set in turn all the parameters but one at $\tau = 0$, and we adjusted the remaining one in order to obtain $A = 2$ s. The results (Table 3) are considered to be upper limits for the lifetimes of the surface intermediates involved in F–T synthesis over ruthenium, which suggests that at the prevailing conditions C–C bond formation over ruthenium is very fast, occurring at a rate exceeding 1 s^{-1}. Whereas compared to our preliminary study (rate exceeding 0.067 s^{-1} (*9*)) we improved significantly on the overall response time of the equipment, the rates over ruthenium are still too fast to be observed, and only lower limits can be quoted. Rates exceeding 1 s^{-1} is also what is being quoted by Mims and McCandlish in their recent transient-kinetic study of F–T over *iron* (*20*).

The concurrent ingrowth of ^{13}C in CH_4 and C_3H_6 demonstrates that in case of ruthenium mass-transfer effects are negligible. As the cobalt preparation has a lower porosity this conclusion carries over to cobalt: the delays observed in Fig. 5 derive from intrinsic rather than extraneous effects.

We utilized in the analysis of the cobalt data two different methods to infer from the transient-kinetic data values for the parameter set τ_b, τ_1, τ_2, and τ_3. In the "leading edge" method we matched the model predictions (Eq. (5)) for the various $F_i = F(^{12}C_{n-i}{}^{13}C_i)$ versus-time-curves against the leading edges ($t \leq \tau_1$) of the experimentally

observed transients. The following results emerge:

(1) The leading edge of the transient $^{13}C_3H_6$ cannot be described satisfactorily by any set τ_b, τ_1, τ_2, and τ_3 which is compatible with the other transients (Fig. 3).

(2) The leading edges for all the other transients are reasonably well reproduced (Figs. 2 and 3) for $\tau_1 = \tau_2 = \tau_3 = 15$ s and $\tau_b \sim 1.5$ s.

(3) Compared to the model predictions the actual transients exhibit significant tailing for $t \geq \tau_1$ (Figs. 3 and 4).

(4) We are unable to reproduce both the "leading edge" ($t \leq \tau_1$) and "tail" ($t \geq \tau_1$) features with a single set τ_b, τ_1, τ_2, and τ_3.

As the τ values quoted above are questionable in the sense that only the leading edges of the transients are being reproduced we derived a second criterion to infer τ values. The alternate criterion consists of a match of the total area (units: s) bounded by the transients, rather than a match of the leading edges. This method leads to essentially the same set of τ values (Table 4). The "leading edge" criterion essentially fulfills the "area" criterion, as an overshoot for $t < \tau_1$ is being compensated by an undershoot for $t > \tau_1$ (Figs. 2 and 3). It is therefore concluded that inferred τ values are rather insensitive toward the fitting criterion. In what follows all values for τ (Fig. 7) and related parameters (Figs. 8 and 9) have been obtained by matching areas rather than leading edges.

Neither the transients (Figs. 1–5) nor the data in Table 4 have been corrected for the (significant) fragmentation accompanying the mass analysis. A further analysis (*29*) indicates that correcting this effect does not remove the "tails" in the transients, and that it does not change the estimates for τ_1 and τ_b. However, the "best fit" values for τ_2 and τ_3 decrease by some 20%.

We conclude that at the prevailing conditions C–C bond formation over cobalt takes place at a rate varying around 0.067 s^{-1} (Fig. 7). With the help of the appropriate relations (Fig. 6):

$$\tau^{-1} = k_p + k_t \tag{6}$$

$$\alpha = \frac{k_p}{k_p + k_t} \tag{7}$$

and

$$\theta_i = \tau_i \cdot \mathrm{TOF}/(1 - \alpha) \tag{8}$$

we obtain the data summarized in Figs. 8 and 9. That we obtain actual numbers for absolute rate constants (k, s^{-1}) and coverages (θ) is, of course, uniquely related to the transient-kinetic nature of the experiments.

When varying the ratio D_2/CO we observe variations in α (Table 2), TOF_i (Table 2), k (Fig. 9), and θ (Fig. 8). However, the lifetime of the surface intermediates:

$$\tau = (k_p + k_t)^{-1}$$

turns out to be highly D_2/CO independent (Fig. 7). Whereas the reaction pathway (i.e., k_p versus k_t and therefore the chain-length parameter α) varies, as expected, with the ratio D_2/CO (Table 2), the overall

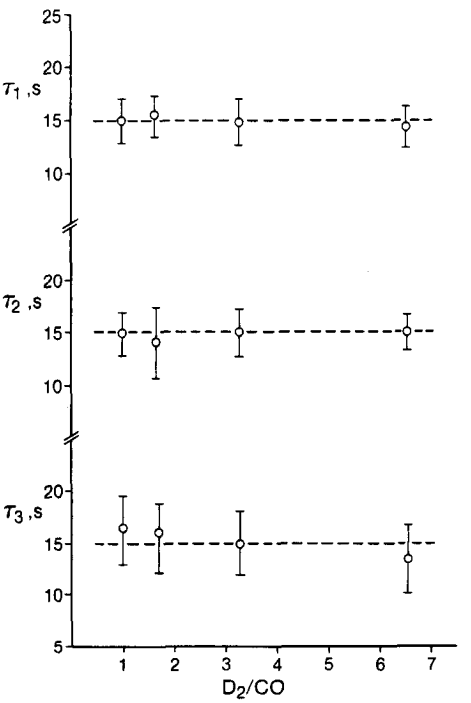

FIG. 7. The τ values at different D_2/CO ratios. T = 210°C, P = 1 bar, catalyst: cobalt.

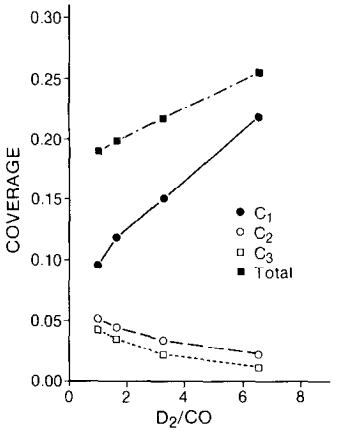

FIG. 8. The θ values at different D_2/CO ratios. T = 210°C, P = 1 bar, catalyst: cobalt.

reactivity, τ, of the growing chains remains virtually constant. This is one of several surprises which, in our appraisal, needs much more transient-kinetic work in order to understand its implications. We merely suggest that this finding could indicate propagation and termination to proceed through a common transition state, with the reaction coordinate leading to this transition state having predominantly the character of a carbon-to-cobalt rather than that of a carbon-to-hydrogen distance.

The transients exhibit "tails" which cannot be accommodated in the simple scheme depicted in Fig. 6. We consider the tails to be indicative of heterogeneity in the pool of intermediates, with the real situation corresponding to a (skewed) distribution of τ values rather than a single τ value per pool. A similar behavior is being reported by Mims and McCandlish (*20*), and in our recent transient-kinetic study of Raney nickel the same phenomena (*28*) was observed. Details in the latter study indicate that heterogeneity of the catalyst itself, as opposed to heterogeneous deterioration of carbonaceous adlayer, underlies the observations.

We finally consider the very short lifetimes of the C_1 building blocks involved in chain growth:

$$C_n + C_b \rightarrow C_{n+1}$$

In the spirit of our own findings (*2*) and those of others (*3–5*) we tend to identify the C_b species with CH_2, and we would expect rapid equilibria such as

$$C_b{=}CH_2 \underset{-H}{\overset{+H}{\rightleftharpoons}} CH_3{=}C_1$$

to cause the pools C_b and C_1 (Fig. 6) to act as a single reservoir, with therefore:

$$\tau_b = \tau_1$$

However, the modeling leads to the surprising result (Table 4):

$$\tau_b \ll \tau_{1,2,3}.$$

How reliable is this modeling result, and what could it convey regarding the nature of the C_b building blocks?

With respect to the veracity of the modeling we mention that our results rest on the following features:

(1) The experimentally observed transients of $^{13}C^{12}CH_4$ and $^{13}C^{12}C_2H_6$ exhibit leading edges which rise simultaneously with that of $^{13}CH_4$ (Figs. 2 and 3).

(2) Modeling has been performed according to Fig. 6, i.e., with all of the CH_4 assigned to reservoir C_1 and without accommodation of surface heterogeneity.

Within these constraints the choice τ_b =

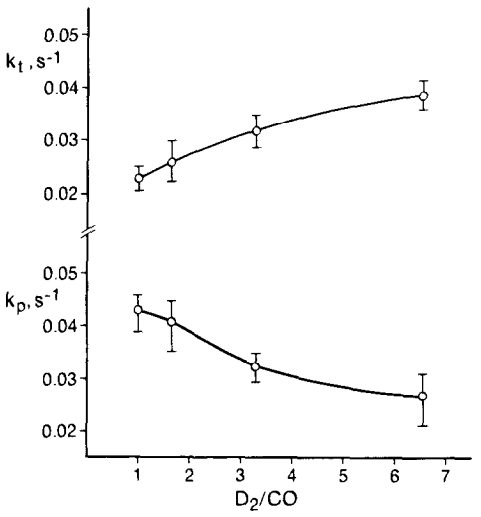

FIG. 9. The k_p and k_t for C_3H_6 at different D_2/CO ratios. T = 210°C, P = 1 bar, catalyst = cobalt.

τ_1 results in a clearcut separation of the leading edges of $^{13}C^{12}CH_4$ and $^{13}C^{12}C_2H_6$, incompatible with observation (1), which is the basis for the quoting $\tau_b \sim 2$ s (Table 4). This leads us to question the validity of the following assumptions made in the modeling:

(a) Assuming growing chains to be started by the same pool of C_1 intermediates which furnish the (excessively produced) CH_4.

(b) Neglecting surface heterogeneity when interpreting the leading-edge features of the transients.

Point (b) is reinforced by the observation that the leading edge of $^{13}C_3H_6$ rises too fast (cf. Fig. 3) to be described by the parameter choice of Table 4. There is every reason to seriously consider too fast a rise, from the experimental point of view, as artifacts are expected to cause spureous delays.

Accommodating a very short lifetime of the C_b building blocks in a chain-growth mechanism would require either unidirectional hydrogenation, as quoted by Happel *et al.* (*16*):

$$\longrightarrow CH_2\ (\tau_b) \xrightarrow{+H} CH_3\ (\tau_1) \longrightarrow$$

or identification of the C_b building blocks with a CO-like species: due to rapid adsorption/desorption the residence time of CO-ad indeed is of the order of 2 s (*9, 21*).

ACKNOWLEDGMENTS

Financial support from the Department of Energy, Office of Fossil Energy (Contract DE-AC22-84PC70020) and from the Exxon Education Foundation is gratefully acknowledged, as is the help of the authors of Ref. (*22*) in making their manuscript available prior to publication.

REFERENCES

1. Vannice, M. A., *Catal. Rev.-Sci. Eng.* **14,** 153 (1976).
2. Biloen, P., and Sachtler, W. M. H., "Advances in Catalysis," Vol. 30, p. 165. Academic Press, New York, 1981.
3. Ponec, V., *Catal. Rev.-Sci. Eng.* **18,** 151 (1982).
4. Ponec, V., *Catalysis* **2,** 49 (1982).
5. Bell, A. T., *Catal. Rev.-Sci. Eng.* **23,** 203 (1981).
6. Feimer, J. L., Silverton, P. L., and Hudgins, R. R., *Canad. J. Chem. Eng.* **62,** 241 (1984).
7. Baker, J. A., and Bell, A. T., *J. Catal.* **78,** 165 (1982).
8. Biloen, P., *J. Mol. Catal.* **21,** 17 (1983).
9. Biloen, P., Helle, J. N., van den Berg, F. G. A., and Sachtler, W. M. H., *J. Catal.* **81,** 450 (1983).
10. Zhang, X. Z., M.S. thesis. University of Pittsburgh, 1985.
11. Herrington, E. F. G., *Chem. Ind. (London)* (1946).
12. Boudart, M., "Kinetics of Chemical Process." Prentice-Hall, Englewood Cliffs, N.J., 1968.
13. Kobayashi, H., and Kobayashi, M., *Catal. Rev.-Sci. Eng.* **10**(2), 139 (1974).
14. Bennett, C. O., *Catal. Rev.-Sci. Eng.* **13**(2), 121 (1976).
15. Tamaru, K., "Dynamic Heterogeneous Catalysis." Academic Press, New York, 1978.
16. Happel, J., Suzuki, I., Kobayeff, P., and Fthenakis, V., *J. Catal.* **65,** 59 (1980).
17. Dautzenberg, F. M., Helle, J. N., van Santen, R. A., and Verbeek, H., *J. Catal.* **50,** 8 (1977).
18. Kieffer, E. Ph., Ph.D. thesis. Technology University, Eindhoven, The Netherlands, 1981.
19. Tamaru, K., *in* "Proceedings, 7th International Conference on Catalysis, Tokyo, 1980," p. 4. Elsevier, Amsterdam, 1980.
20. Mims, C. A., and McCandlish, L. E., *J. Amer. Chem. Soc.* **107,** 696 (1985).
21. Yang, C. H., Soong, Y., and Biloen, P., *in* "Proceedings, 8th International Congress on Catalysis, Berlin, II-3, 1984."
22. Biloen, P., Helle, J. N., and Sachtler, W. M. H., *J. Catal.* **58,** 95 (1979).
23. Brady, R. C., and Pettit, R. J., *J. Amer. Chem. Soc.* **102,** 6181 (1980).
24. Brady, R. C., and Pettit, R. J., *J. Amer. Chem. Soc.* **103,** 1287 (1981).
25. Bonzel, H. P., and Krebs, H. J., *Surf. Sci.* **91,** 499 (1980).
26. McCarty, J. G., and Wise, H., *J. Catal.* **57,** 406 (1979).
27. Goodman, D. W., Kelley, R. D., Madey, T. E., and White, J. M., *J. Catal.* **64,** 479 (1980).
28. Soong, Y., and Biloen, P., *J. Catal.* in press.
29. Zhang, X. Z., and Biloen, P., in preparation.